

# Continuous variable tripartite entanglement from twin nonlinearities

M K Olsen and A S Bradley

ARC Centre of Excellence for Quantum-Atom Optics, School of Physical Sciences,  
University of Queensland, Brisbane 4072, Qld, Australia

E-mail: [mko@physics.uq.edu.au](mailto:mko@physics.uq.edu.au)

Received 16 September 2005, in final form 4 November 2005

Published 5 December 2005

Online at [stacks.iop.org/JPhysB/39/127](http://stacks.iop.org/JPhysB/39/127)

## Abstract

In this work, we analyse and compare the continuous variable tripartite entanglement available from the use of two concurrent or cascaded  $\chi^{(2)}$  nonlinearities. We examine both idealized travelling-wave models and more experimentally realistic intracavity models, showing that tripartite entangled outputs are readily producible. These may be a useful resource for applications such as quantum cryptography and teleportation.

(Some figures in this article are in colour only in the electronic version)

## 1. Introduction

Entanglement is a property which is central to quantum mechanics, with continuous variable bipartite entanglement being readily producible experimentally. A two-mode system is considered to be bipartite entangled if the system density matrix cannot be expressed as a product of the density matrices of each of the two modes. The definition of tripartite entanglement for three-mode systems is a little more subtle, with different classes of entanglement having been defined, depending on how the system density matrix may be partitioned [1]. The classifications range from fully inseparable, which means that the density matrix is not separable for any grouping of the modes, to fully separable, where the three modes are not entangled in any way. For the fully inseparable case, van Loock and Furusawa [2], who call this genuine tripartite entanglement, have derived inequalities which are easily applicable to continuous variable processes. These are the inequalities which we shall evaluate in this work.

While there has been some experimental progress in the production of tripartite entangled beams, this entanglement is often obtained by mixing squeezed vacua with linear optical elements [3, 4]. Other methods which create the entanglement in the actual nonlinear interaction have been proposed, using both cascaded and concurrent  $\chi^{(2)}$  processes [5–7]. In this paper, we investigate the fundamental limits to the achievable tripartite entanglement

available from two processes which utilize twin nonlinearities in the concurrent and cascaded configurations. We evaluate the continuous variable tripartite entanglement criteria of van Loock and Furusawa [2] for two different interaction Hamiltonians and then calculate the performance of the corresponding intracavity systems which contain the interactions described by these Hamiltonians. We will show that fully inseparable tripartite entanglement is predicted for a range of parameters.

## 2. Criteria for tripartite entanglement

We will first describe the inequalities whose violation is sufficient to demonstrate that a system demonstrates true continuous variable tripartite entanglement. For three modes described by the annihilation operators  $\hat{a}_j$ , where  $j = 1, 2, 3$ , we define quadrature operators for each mode as

$$\hat{X}_j = \hat{a}_j + \hat{a}_j^\dagger, \quad \hat{Y}_j = -i(\hat{a}_j - \hat{a}_j^\dagger), \quad (1)$$

so that the Heisenberg uncertainty principle requires  $V(\hat{X}_j)V(\hat{Y}_j) \geq 1$ . A set of conditions which are sufficient to demonstrate tripartite entanglement have been derived by van Loock and Furusawa [2], without making any assumptions about Gaussian statistics. Note that a set of conditions often used to demonstrate continuous variable bipartite entanglement, which were developed by Duan *et al* using the properties of the covariance matrix [8] (see also [9]), are both necessary and sufficient for Gaussian variables.

The general van Loock–Furusawa inequalities are expressed in terms of linear combinations of the quadrature operators. In this work, we will confine our attention to a particular linear combination (corresponding to  $h_1 = g_1 = g_2 = g_3 = 1 = -h_2$  and  $h_3 = 0$  in the van Loock–Furusawa notation). This choice leads to symmetric conditions for modes  $i$  and  $j$  to be separable, so that each inequality actually addresses the separability of two modes. Using these operator combinations and our quadrature definitions, the van Loock and Furusawa conditions give a set of inequalities,

$$\begin{aligned} V_{12} &= V(\hat{X}_1 - \hat{X}_2) + V(\hat{Y}_1 + \hat{Y}_2 + \hat{Y}_3) \geq 4, \\ V_{13} &= V(\hat{X}_1 - \hat{X}_3) + V(\hat{Y}_1 + \hat{Y}_2 + \hat{Y}_3) \geq 4, \\ V_{23} &= V(\hat{X}_2 - \hat{X}_3) + V(\hat{Y}_1 + \hat{Y}_2 + \hat{Y}_3) \geq 4, \end{aligned} \quad (2)$$

where  $V(A) \equiv \langle A^2 \rangle - \langle A \rangle^2$ . As shown in [2], the violation of the first condition still leaves the possibility that mode 3 could be separated from modes 1 and 2, but this possibility is negated by violation of the second inequality. Starting with any one of the conditions thus shows that, if any two of these inequalities are violated, the system is fully inseparable and genuine tripartite entanglement is guaranteed. We note that genuine tripartite entanglement may still be possible when none of these inequalities is violated, due to the criteria being sufficient but not necessary.

We note here that, although states which violate these inequalities are sometimes called continuous variable GHZ states, actual GHZ states rely on perfect correlations [10, 11]. This terminology would be accurate if the states involved were eigenstates of amplitude quadrature differences and phase quadrature sums. This would, however, require infinite squeezing of the electromagnetic field which in turn would require infinite energy. As this is physically impossible, we will not use the GHZ terminology in this paper.

### 3. Travelling-wave models

In this section, we will examine simplified models of two processes which utilize two concurrent or cascaded nonlinearities to produce tripartite entanglement. We will proceed by solving both stochastic equations which are equivalent to the Heisenberg equations of motion derived from the interaction Hamiltonians and approximate operator equations obtained by ignoring pump depletion. While these procedures are not intended to model realistic physical processes with propagating waves, which would need a more complicated treatment [12], they do give some idea of the degree of entanglement available from these Hamiltonians. In the next section, we will perform more realistic analyses of the same processes inside pumped optical cavities.

#### 3.1. Two cascaded nonlinearities

Ferraro *et al* have proposed a linked nonlinear process which links five different modes [6] and was first investigated in terms of photon statistics by Smithers and Lu [13]. It has recently been analysed in terms of its nonlocal properties by Ferraro and Paris [14], with the theoretical analyses of all these works using the undepleted pump approximation. However, it is known that the squeezing and bipartite entanglement in travelling-wave  $\chi^{(2)}$  processes do not become perfect as the interaction strength increases, but reach some finite limit and then decrease [15–17]. We will therefore quantize the pump modes and analyse this system using the full stochastic equations of motion, which must be done numerically. The process involves modes which we will describe using the operators  $\hat{b}_1(\omega_1)$ ,  $\hat{b}_2(\omega_2)$ ,  $\hat{a}_1(\omega_3)$ ,  $\hat{a}_2(\omega_4)$  and  $\hat{a}_3(\omega_5)$  where the frequencies obey

$$\omega_1 = \omega_3 + \omega_4, \quad \omega_5 = \omega_2 + \omega_4. \quad (3)$$

The interaction Hamiltonian can then be written as

$$H_{\text{int}} = i\hbar(\chi_1 \hat{b}_1^\dagger \hat{a}_1 \hat{a}_2 + \chi_2 \hat{b}_2^\dagger \hat{a}_2^\dagger \hat{a}_3) + \text{h.c.}, \quad (4)$$

which we see describes the same process as [6], once all the interacting fields are quantized. Note that we have changed the indices of modes 2 and 3 compared with those used by Ferraro *et al*, so that both our 1 and 2 are produced by the  $\chi_1$  interaction. This Hamiltonian describes a downconversion process cascaded with a sum-frequency generation process where one of the downconverted modes becomes a pump mode for the frequency generation process.

Before we develop and investigate the full equations from (4), it is instructive to examine the analytical solutions which may be obtained using an undepleted pump approximation. Setting  $\kappa_1 = \chi_1 \langle \hat{b}_1(0) \rangle$  and  $\kappa_2 = \chi_2 \langle \hat{b}_2(0) \rangle$  as real positive constants, we find the Heisenberg equations of motion,

$$\frac{d\hat{a}_1}{dt} = \kappa_1 \hat{a}_2^\dagger, \quad \frac{d\hat{a}_2}{dt} = \kappa_1 \hat{a}_1^\dagger - \kappa_2 \hat{a}_3, \quad \frac{d\hat{a}_3}{dt} = \kappa_2 \hat{a}_2. \quad (5)$$

We find that there are two classes of solutions, depending on whether  $\kappa_2^2 > \kappa_1^2$  or  $\kappa_2^2 < \kappa_1^2$ . In the first case, where  $\kappa_2^2 > \kappa_1^2$ , we set  $\Omega = \sqrt{\kappa_2^2 - \kappa_1^2}$  to find

$$\begin{aligned} \hat{a}_1(t) &= \frac{\kappa_2^2 - \kappa_1^2 \cos \Omega t}{\Omega^2} \hat{a}_1(0) + \frac{\kappa_1 \sin \Omega t}{\Omega} \hat{a}_2^\dagger(0) + \frac{\kappa_1 \kappa_2 (\cos \Omega t - 1)}{\Omega^2} \hat{a}_3^\dagger(0), \\ \hat{a}_2(t) &= \frac{\kappa_1 \sin \Omega t}{\Omega} \hat{a}_1^\dagger(0) + \hat{a}_2(0) \cos \Omega t - \frac{\kappa_2 \sin \Omega t}{\Omega} \hat{a}_3(0), \\ \hat{a}_3(t) &= \frac{\kappa_1 \kappa_2 (1 - \cos \Omega t)}{\Omega^2} \hat{a}_1^\dagger(0) + \frac{\kappa_2 \sin \Omega t}{\Omega} \hat{a}_2(0) + \frac{\kappa_2^2 \cos \Omega t - \kappa_1^2}{\Omega^2} \hat{a}_3(0), \end{aligned} \quad (6)$$

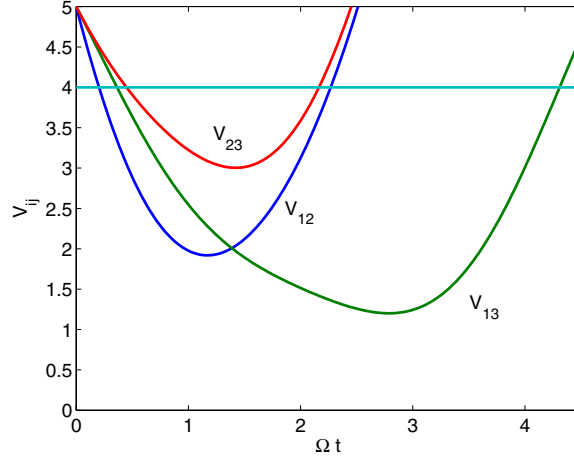


**Figure 1.** The analytical solutions of the van Loock–Furusawa correlations for the Ferraro scheme, with  $\kappa_2 = 1.8\kappa_1$ . Any two of the correlations falling below 4 are sufficient to demonstrate that genuine tripartite entanglement is present.

which, beginning with all the  $a$  modes initially as vacuum, gives the solutions for the intensities as

$$\langle \hat{a}_2^\dagger \hat{a}_2 \rangle = \frac{\kappa_1^2 \sin^2 \Omega t}{\Omega^2}, \quad \langle \hat{a}_3^\dagger \hat{a}_3 \rangle = \frac{\kappa_1^2 \kappa_2^2 (\cos \Omega t - 1)^2}{\Omega^4}, \quad \langle \hat{a}_1^\dagger \hat{a}_1 \rangle = \langle \hat{a}_2^\dagger \hat{a}_2 \rangle + \langle \hat{a}_3^\dagger \hat{a}_3 \rangle. \quad (7)$$

We see that these are the same as the analytical solutions given by Ferraro *et al* [6], once the change of indices is taken into account.

We can use the solutions of (6) to find expressions for the quadrature variances and covariances,

$$\begin{aligned} V(\hat{X}_1) = V(\hat{Y}_1) &= 1 + \frac{4\kappa_1^2 \kappa_2^2 (1 - \cos \Omega t) - 2\kappa_1^4 \sin^2 \Omega t}{\Omega^4}, \\ V(\hat{X}_2) = V(\hat{Y}_2) &= 1 + \frac{2\kappa_1^2 \sin^2 \Omega t}{\Omega^2}, \\ V(\hat{X}_3) = V(\hat{Y}_3) &= 1 + \frac{2\kappa_1^2 \kappa_2^2 (1 - \cos \Omega t)^2}{\Omega^4}, \\ V(\hat{X}_1, \hat{X}_2) = -V(\hat{Y}_1, \hat{Y}_2) &= \frac{2\kappa_1 \sin \Omega t}{\Omega^3} (\kappa_2^2 - \kappa_1^2 \cos \Omega t), \\ V(\hat{X}_1, \hat{X}_3) = -V(\hat{Y}_1, \hat{Y}_3) &= \frac{2\kappa_1 \kappa_2}{\Omega^4} [\kappa_1^2 \cos^2 \Omega t + \kappa_2^2 - (\kappa_1^2 + \kappa_2^2) \cos \Omega t], \\ V(\hat{X}_2, \hat{X}_3) = V(\hat{Y}_2, \hat{Y}_3) &= \frac{2\kappa_1^2 \kappa_2}{\Omega^3} \sin \Omega t (1 - \cos \Omega t). \end{aligned} \quad (8)$$

These expressions contain all the information necessary to express the van Loock–Furusawa correlations, since  $V(\hat{X}_i - \hat{X}_j) = V(\hat{X}_i) + V(\hat{X}_j) - 2V(\hat{X}_i, \hat{X}_j)$  and  $V(\hat{Y}_1 + \hat{Y}_2 + \hat{Y}_3) = V(\hat{Y}_1) + V(\hat{Y}_2) + V(\hat{Y}_3) + 2(V(\hat{Y}_1, \hat{Y}_2) + V(\hat{Y}_1, \hat{Y}_3) + V(\hat{Y}_2, \hat{Y}_3))$ . The expressions for the van Loock–Furusawa correlations obtained by combining these variances and covariances are shown in figure 1, for  $\kappa_2 = 1.8\kappa_1$ . We see that this Hamiltonian provides tripartite entanglement over a range of scaled interaction time.

If  $\kappa_1^2 > \kappa_2^2$ , the solutions are not periodic so that the undepleted pump approximation is of limited validity, being expected to give accurate answers only for short times. However,

setting  $\zeta = \sqrt{\kappa_1^2 - \kappa_2^2}$ , we find

$$\begin{aligned}\hat{a}_1(t) &= \frac{\kappa_1^2 \cosh \zeta t - \kappa_2^2}{\zeta^2} \hat{a}_1(0) + \frac{\kappa_1 \sinh \zeta t}{\zeta} \hat{a}_2^\dagger(0) + \frac{\kappa_1 \kappa_2 (1 - \cosh \zeta t)}{\zeta^2} \hat{a}_3^\dagger(0), \\ \hat{a}_2(t) &= \frac{\kappa_1 \sinh \zeta t}{\zeta} \hat{a}_1^\dagger(0) + \hat{a}_2(0) \cosh \zeta t - \frac{\kappa_2 \sinh \zeta t}{\zeta} \hat{a}_3(0), \\ \hat{a}_3(t) &= \frac{\kappa_1 \kappa_2 (\cosh \zeta t - 1)}{\zeta^2} \hat{a}_1^\dagger(0) + \frac{\kappa_2 \sinh \zeta t}{\zeta} \hat{a}_2(0) + \frac{\kappa_1^2 - \kappa_2^2 \cosh \zeta t}{\zeta^2} \hat{a}_3(0),\end{aligned}\tag{9}$$

with the mean intensities being, again with these modes beginning as vacuum,

$$\langle \hat{a}_2^\dagger \hat{a}_2 \rangle = \frac{\kappa_1^2 \sinh^2 \zeta t}{\zeta^2}, \quad \langle \hat{a}_3^\dagger \hat{a}_3 \rangle = \frac{\kappa_1^2 \kappa_2^2 (\cosh \zeta t - 1)^2}{\zeta^4}, \quad \langle \hat{a}_1^\dagger \hat{a}_1 \rangle = \langle \hat{a}_2^\dagger \hat{a}_2 \rangle + \langle \hat{a}_3^\dagger \hat{a}_3 \rangle.\tag{10}$$

We note here that these solutions have previously been given by Smithers and Lu [13] and that we have presented them here because we intend to use them to find analytical expressions for the correlation functions of interest. In this case, the solutions for the variances and covariances are found as

$$\begin{aligned}V(\hat{X}_1) &= V(\hat{Y}_1) = 1 + \frac{2\kappa_1^2 [\kappa_1^2 \sinh^2 \zeta t + \kappa_2^2 (2 - 2 \cosh \zeta t)]}{\zeta^4}, \\ V(\hat{X}_2) &= V(\hat{Y}_2) = 1 + \frac{2\kappa_1^2 \sinh^2 \zeta t}{\zeta^2}, \\ V(\hat{X}_3) &= V(\hat{Y}_3) = 1 + \frac{2\kappa_1^2 \kappa_2^2 (\cosh \zeta t - 1)^2}{\zeta^4}, \\ V(\hat{X}_1, \hat{X}_2) &= -V(\hat{Y}_1, \hat{Y}_2) = \frac{2\kappa_1 \sinh \zeta t}{\zeta^3} (\kappa_1^2 \cosh \zeta t - \kappa_2^2), \\ V(\hat{X}_1, \hat{X}_3) &= -V(\hat{Y}_1, \hat{Y}_3) = \frac{2\kappa_1 \kappa_2}{\zeta^4} [(\kappa_1^2 + \kappa_2^2)(1 - \cosh \zeta t) + \kappa_1^2 \cosh^2 \zeta t], \\ V(\hat{X}_2, \hat{X}_3) &= V(\hat{Y}_2, \hat{Y}_3) = \frac{2\kappa_1^2 \kappa_2}{\zeta^3} \sinh \zeta t (\cosh \zeta t - 1).\end{aligned}\tag{11}$$

The system also exhibits tripartite entanglement in this regime, as can be seen in figure 2. However, as the solutions for the intensities are hyperbolic, they quickly increase to the point where the undepleted pump approximation will lose its validity. Neither of the analytic treatments used above is useful for the case where  $\kappa_1^2 = \kappa_2^2$ , for which we will employ stochastic integration.

In developing our full equations of motion, we will follow the approach of Huttner *et al* [18] (see also [19]) treating the interacting fields in terms of the photon fluxes rather than in terms of energy densities. As stated in [18], this approach avoids problems which could arise, especially with the quantization volume, if we were to work with the normal Hamiltonian approach. With the appropriate momentum-space operators, we use the well-known mapping onto stochastic differential equations in the positive- $P$  representation [20] to calculate the development of the fields as they traverse the medium. We note here that this phase-space representation allows for an exact and complete mapping of our Hamiltonian onto stochastic differential equations. We consider here the case of one-dimensional propagation, which is valid for the case of collinear pumping. We also note here that this approach assumes that the medium is not dispersive for the interacting fields, which is a difficult condition to meet with existing materials. In this approach, the operator

$$\hat{N}(z_0, \omega_m) \equiv \hat{a}^\dagger(z_0, \omega_m) \hat{a}(z_0, \omega_m),\tag{12}$$

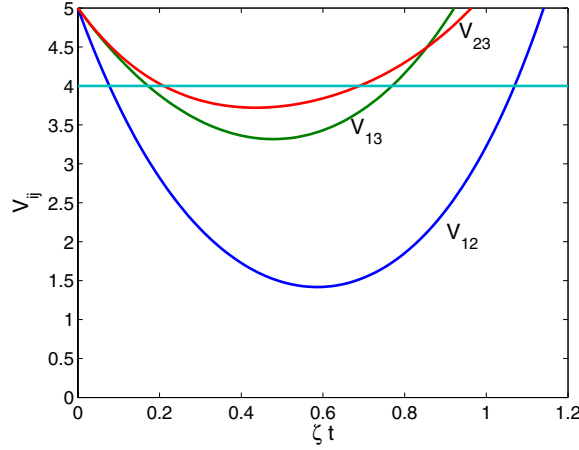


**Figure 2.** The analytical solutions of the van Loock–Furusawa correlations for the Ferarro scheme, with  $\kappa_1 = 1.2\kappa_2$ . Any two of the correlations falling below 4 are sufficient to demonstrate that genuine tripartite entanglement is present.

for example, is the number operator for photons at frequency  $\omega_m$  which pass through a plane at  $z = z_0$  during a chosen time interval. The operators  $\hat{a}^\dagger(z, \omega_m)$  and  $\hat{a}(z, \omega_m)$  then obey bosonic spatial commutation relations,

$$[\hat{a}(z, \omega_i), \hat{a}^\dagger(z', \omega_j)] = \delta_{ij}\delta(z - z'), \quad (13)$$

and similarly for the  $\hat{b}_j$  operators. The nonlinear momentum operator for this system is found as

$$\hat{G}_{nl}(z) = i\hbar(\chi_1 \hat{b}_1^\dagger \hat{a}_1 \hat{a}_2 + \chi_2 \hat{b}_2^\dagger \hat{a}_2^\dagger \hat{a}_3) + \text{h.c.} \quad (14)$$

As shown by Shen [21], we can write an equation of motion for the density matrix of the system,

$$i\hbar \frac{\partial \rho(z)}{\partial z} = [\rho(z), \hat{G}_{nl}(z)], \quad (15)$$

which allows for the calculation of steady-state propagation, exactly as required for continuous pumping. Physically, the density matrix,  $\rho(z)$ , describes an ensemble of steady-state systems which has all the statistical properties of the fields at point  $z$ . Equation (15) provides a full description of the interacting fields of our model, but is extremely difficult to solve directly.

Therefore, following the standard procedures [22], we map the master equation onto the Fokker–Planck equation for the positive- $P$  pseudoprobability distribution,

$$\begin{aligned} \frac{dP}{dz} = & \left\{ - \left[ \frac{\partial}{\partial \alpha_1} \chi_1 \alpha_2^+ \beta_1 + \frac{\partial}{\partial \alpha_1^+} \chi_1 \alpha_2 \beta_1^+ + \frac{\partial}{\partial \alpha_2} (\chi_1 \alpha_1^+ \beta_1 - \chi_2 \alpha_3 \beta_2^+) + \frac{\partial}{\partial \alpha_2^+} (\chi_1 \alpha_1 \beta_1^+ - \chi_2 \alpha_3^+ \beta_2) \right. \right. \\ & + \frac{\partial}{\partial \alpha_3} \chi_2 \alpha_2 \beta_2 + \frac{\partial}{\partial \alpha_3^+} \chi_2 \alpha_2^+ \beta_2^+ + \frac{\partial}{\partial \beta_1} (-\chi_1 \alpha_1 \alpha_2) + \frac{\partial}{\partial \beta_1^+} (-\chi_1 \alpha_1^+ \alpha_2^+) \\ & \left. \left. + \frac{\partial}{\partial \beta_2} (-\chi_2 \alpha_2 \alpha_3^+) + \frac{\partial}{\partial \beta_2^+} (-\chi_2 \alpha_2^+ \alpha_3) \right] + \frac{1}{2} \left[ \frac{\partial^2}{\partial \alpha_1 \partial \alpha_2} 2\chi_1 \beta_1 + \frac{\partial^2}{\partial \alpha_1^+ \partial \alpha_2^+} 2\chi_1 \beta_1^+ \right. \right. \\ & \left. \left. - \frac{\partial^2}{\partial \alpha_2 \partial \beta_2} 2\chi_2 \alpha_3 - \frac{\partial^2}{\partial \alpha_2^+ \partial \beta_2^+} 2\chi_2 \alpha_3^+ \right] \right\} P(\tilde{\alpha}, z), \quad (16) \end{aligned}$$

where  $\tilde{\alpha} = (\alpha_1, \alpha_1^+, \alpha_2, \alpha_2^+, \alpha_3, \alpha_3^+, \beta_1, \beta_1^+, \beta_2, \beta_2^+)$ . As always with the positive- $P$  representation, stochastic averages of products of the variables represent normally ordered operator expectation values, with there being correspondences between  $\alpha_j, \alpha_j^+, \beta_j, \beta_j^+$  and  $\hat{a}_j, \hat{a}_j^\dagger, \hat{b}_j, \hat{b}_j^\dagger$ . We now map this Fokker–Planck equation onto the following set of stochastic differential equations in Itô calculus:

$$\begin{aligned}
\frac{d\alpha_1}{dz} &= \chi_1 \alpha_2^+ \beta_1 + \sqrt{\frac{\chi_1 \beta_1}{2}} (\eta_1 + i\eta_3), \\
\frac{d\alpha_1^+}{dz} &= \chi_1 \alpha_2 \beta_1^+ + \sqrt{\frac{\chi_1 \beta_1^+}{2}} (\eta_2 + i\eta_4), \\
\frac{d\alpha_2}{dz} &= \chi_1 \alpha_1^+ \beta_1 - \chi_2 \alpha_3 \beta_2^+ + \sqrt{\frac{\chi_1 \beta_1}{2}} (\eta_1 - i\eta_3) - \sqrt{\frac{\chi_2 \alpha_3}{2}} (\eta_7 - i\eta_5), \\
\frac{d\alpha_2^+}{dz} &= \chi_1 \alpha_1 \beta_1^+ - \chi_2 \alpha_3^+ \beta_2 + \sqrt{\frac{\chi_1 \beta_1^+}{2}} (\eta_2 - i\eta_4) - \sqrt{\frac{\chi_2 \alpha_3^+}{2}} (\eta_8 - i\eta_6), \\
\frac{d\alpha_3}{dz} &= \chi_2 \alpha_2 \beta_2, \\
\frac{d\alpha_3^+}{dz} &= \chi_2 \alpha_2^+ \beta_2^+, \\
\frac{d\beta_1}{dz} &= -\chi_1 \alpha_1 \alpha_2, \\
\frac{d\beta_1^+}{dz} &= -\chi_1 \alpha_1^+ \alpha_2^+, \\
\frac{d\beta_2}{dz} &= -\chi_2 \alpha_2 \alpha_3^+ + \sqrt{\frac{\chi_2 \alpha_3}{2}} (\eta_7 + i\eta_5), \\
\frac{d\beta_2^+}{dz} &= -\chi_2 \alpha_2^+ \alpha_3 + \sqrt{\frac{\chi_2 \alpha_3^+}{2}} (\eta_8 + i\eta_6),
\end{aligned} \tag{17}$$

which we may solve using stochastic integration. The real Gaussian noise terms have the correlations

$$\overline{\eta_j(z)} = 0, \quad \overline{\eta_j(z) \eta_k(z')} = \delta_{jk} \delta(z - z'). \tag{18}$$

The results of stochastic integration in two different parameter regimes are presented in figures 3–5. All show genuine tripartite entanglement over some interaction range and all begin with the output modes as vacuum. For the parameters used in figure 3, with  $\chi_1 \beta_1(0) = \chi_2 \beta_2(0)$ , the output intensities increase monotonically over the range shown and the entanglement disappears. This is unlike the situation of figure 4, where  $\chi_2 \beta_2(0) = 2\chi_1 \beta_1(0)$ , and both the output fields and the van Loock–Furusawa correlations oscillate over a short interaction length. Although the field intensities for the first situation obviously cannot increase indefinitely, this contrast between monotonically increasing and periodic behaviour of the intensities, depending on the ratios of the pumping and interaction strengths, was mentioned by Smithers and Lu [13].

### 3.2. Two concurrent nonlinearities

Another possibility for a travelling-wave model is to have a single crystal with two concurrent nonlinearities, each pumped by different modes. This could be achieved either with different polarizations or with different frequencies. In this section, we will consider a crystal which is pumped at frequencies  $\omega_1$  and  $\omega_2$  to produce modes at  $\omega_3, \omega_4$  and  $\omega_5$ ,

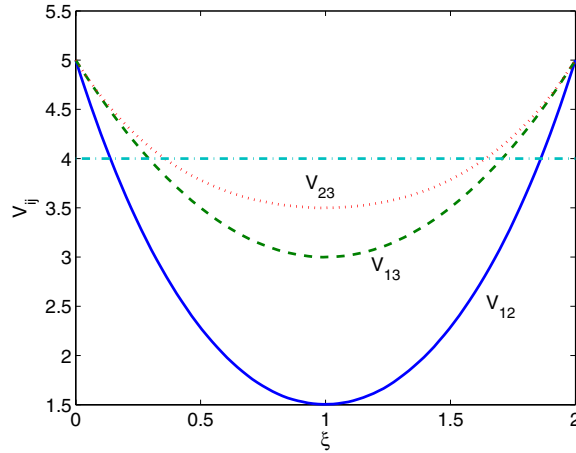


**Figure 3.** The scheme of [6] with everything symmetric,  $\beta_1(0) = \beta_2(0) = 10^3$  and  $\chi_1 = \chi_2 = 10^{-2}$ , averaged over  $1.06 \times 10^6$  stochastic trajectories. The horizontal axis is the scaled interaction length,  $\xi = |\beta_0|\chi z$ . Any two of the correlations falling below 4 are sufficient to demonstrate that genuine tripartite entanglement is present.

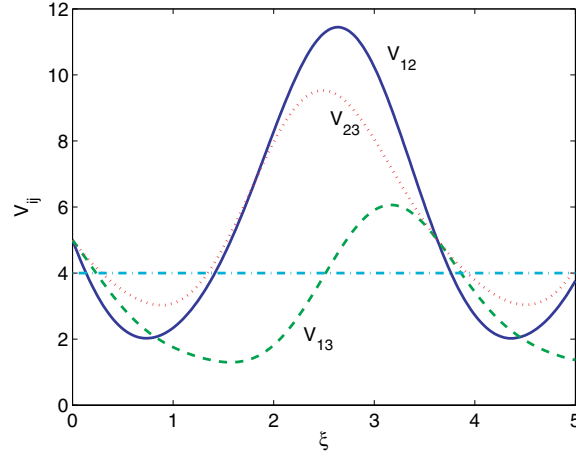


**Figure 4.** The scheme of [6] as in figure 3, but with  $\chi_2 = 2\chi_1$ , averaged over  $3.35 \times 10^6$  stochastic trajectories.

where  $\omega_1 = \omega_3 + \omega_4$  and  $\omega_2 = \omega_4 + \omega_5$ . With all modes quantized with the operators  $\hat{b}_1(\omega_1), \hat{b}_2(\omega_2), \hat{a}_1(\omega_3), \hat{a}_2(\omega_4), \hat{a}_3(\omega_5)$ , the interaction Hamiltonian for this scheme becomes

$$H_{\text{int}} = i\hbar(\chi_1 \hat{b}_1 \hat{a}_1^\dagger \hat{a}_2^\dagger + \chi_2 \hat{b}_2 \hat{a}_2^\dagger \hat{a}_3^\dagger) + \text{h.c.}, \quad (19)$$

where  $\chi_j$  represent the nonlinear interactions.

We will first examine a simplified analytical model for the propagation of fields described by this Hamiltonian. Assuming perfect phase matching and ignoring pump depletion, we may set  $\gamma_1 = \chi_1 \langle \hat{b}_1(0) \rangle$  and  $\gamma_2 = \chi_2 \langle \hat{b}_2(0) \rangle$ , where the pump fields are initially intense coherent states, to find the Heisenberg equations of motion,

$$\frac{d\hat{a}_1}{dt} = \gamma_1 \hat{a}_2^\dagger, \quad \frac{d\hat{a}_2}{dt} = \gamma_1 \hat{a}_1^\dagger + \gamma_2 \hat{a}_3^\dagger, \quad \frac{d\hat{a}_3}{dt} = \gamma_2 \hat{a}_2^\dagger. \quad (20)$$

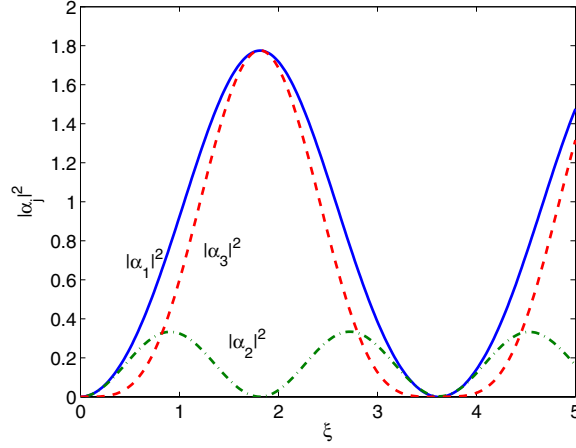


**Figure 5.** The intensities produced by the interaction of the scheme of [6] for the same parameters as used in figure 4.

Setting  $\Omega = \sqrt{\gamma_1^2 + \gamma_2^2}$ , we may solve these linear operator equations to find the solutions

$$\begin{aligned}\hat{a}_1(t) &= \hat{a}_1(0) \frac{\gamma_2^2 + \gamma_1^2 \cosh \Omega t}{\Omega^2} + \hat{a}_2^\dagger(0) \frac{\gamma_1 \sinh \Omega t}{\Omega} + \hat{a}_3(0) \frac{\gamma_1 \gamma_2 (\cosh \Omega t - 1)}{\Omega^2}, \\ \hat{a}_2(t) &= \hat{a}_1^\dagger(0) \frac{\gamma_1 \sinh \Omega t}{\Omega} + \hat{a}_2(0) \cosh \Omega t + \hat{a}_3^\dagger(0) \frac{\gamma_2 \sinh \Omega t}{\Omega}, \\ \hat{a}_3(t) &= \hat{a}_1(0) \frac{\gamma_1 \gamma_2 (\cosh \Omega t - 1)}{\Omega^2} + \hat{a}_2^\dagger(0) \frac{\gamma_2 \sinh \Omega t}{\Omega} + \hat{a}_3(0) \frac{\gamma_1^2 + \gamma_2^2 \cosh \Omega t}{\Omega^2},\end{aligned}\quad (21)$$

which contain all the information required to calculate the desired correlations. With all the output modes initially vacuum, we find the average intensities

$$\langle \hat{a}_1^\dagger \hat{a}_1 \rangle = \frac{\gamma_1^2 \sinh^2 \Omega t}{\Omega^2}, \quad \langle \hat{a}_2^\dagger \hat{a}_2 \rangle = \sinh^2 \Omega t, \quad \langle \hat{a}_3^\dagger \hat{a}_3 \rangle = \frac{\gamma_2^2 \sinh^2 \Omega t}{\Omega^2}, \quad (22)$$

with the variances and covariances for the quadratures being found as

$$\begin{aligned}V(\hat{X}_1) &= V(\hat{Y}_1) = 1 + 2 \frac{\gamma_1^2 \sinh^2 \Omega t}{\Omega^2}, \\ V(\hat{X}_2) &= V(\hat{Y}_2) = 1 + 2 \sinh^2 \Omega t, \\ V(\hat{X}_3) &= V(\hat{Y}_3) = 1 + 2 \frac{\gamma_2^2 \sinh^2 \Omega t}{\Omega^2}, \\ V(\hat{X}_1, \hat{X}_2) &= -V(\hat{Y}_1, \hat{Y}_2) = \frac{\gamma_1 \sinh 2\Omega t}{\Omega}, \\ V(\hat{X}_1, \hat{X}_3) &= V(\hat{Y}_1, \hat{Y}_3) = \frac{2\gamma_1 \gamma_2 \sinh^2 \Omega t}{\Omega^2}, \\ V(\hat{X}_2, \hat{X}_3) &= -V(\hat{Y}_2, \hat{Y}_3) = \frac{\gamma_2 \sinh 2\Omega t}{\Omega}.\end{aligned}\quad (23)$$

We can now calculate the van Loock–Furusawa correlations, finding

$$\begin{aligned}
V(\hat{X}_1 - \hat{X}_2) &= 2 \left[ 1 + \left( 1 + \frac{\gamma_1^2}{\Omega^2} \right) \sinh^2 \Omega t - \frac{\gamma_1}{\Omega} \sinh 2\Omega t \right], \\
V(\hat{X}_1 - \hat{X}_3) &= 2 \left[ 1 + \left( 1 - \frac{2\gamma_1\gamma_2}{\Omega^2} \right) \sinh^2 \Omega t \right], \\
V(\hat{X}_2 - \hat{X}_3) &= 2 \left[ 1 + \left( 1 + \frac{\gamma_2^2}{\Omega^2} \right) \sinh^2 \Omega t - \frac{\gamma_2}{\Omega} \sinh 2\Omega t \right], \\
V(\hat{Y}_1 + \hat{Y}_2 + \hat{Y}_3) &= 3 + \left( 4 + \frac{4\gamma_1\gamma_2}{\Omega^2} \right) \sinh^2 \Omega t - \frac{2(\gamma_1 + \gamma_2)}{\Omega} \sinh 2\Omega t,
\end{aligned} \tag{24}$$

which, for  $\gamma_1 = \gamma_2 = \gamma$ , simplify to give

$$\begin{aligned}
V_{12} &= V_{23} = 5 + 9 \sinh^2 \Omega t - 3\sqrt{2} \sinh 2\Omega t, \\
V_{13} &= 5 + 6 \sinh^2 \Omega t - 2\sqrt{2} \sinh 2\Omega t,
\end{aligned} \tag{25}$$

from which we can see that tripartite entanglement is definitely present for shortish interaction times, but does not increase with  $\Omega t$ . In fact, the minimum of  $V_{12}$  and  $V_{23}$  is found at  $\Omega t = \cosh^{-1} \sqrt{2}$  and has a value of 2.

We will now turn to stochastic integration of the full equations, without using the undepleted pump approximation. In what follows, we will set the interaction strengths equal,  $\chi_1 = \chi_2 = \chi$ , as these are the conditions which give the maximum violation of the inequalities for this system. We define the nonlinear momentum operator for this process as

$$\hat{G}_{nl}(z) = i\hbar \chi (\hat{b}_1^\dagger \hat{a}_1 \hat{a}_2 + \hat{b}_2^\dagger \hat{a}_2 \hat{a}_3) + \text{h.c.} \tag{26}$$

From this operator we may make a mapping onto a Fokker–Planck equation for the positive- $P$  pseudoprobability distribution, from which we find the Itô stochastic differential equations,

$$\begin{aligned}
\frac{d\alpha_1}{dz} &= \chi \alpha_2^+ \beta_1 + \sqrt{\frac{\chi \beta_1}{2}} (\eta_1 + i\eta_6), \\
\frac{d\alpha_1^+}{dz} &= \chi \alpha_2 \beta_1^+ + \sqrt{\frac{\chi \beta_1^+}{2}} (\eta_2 - i\eta_5), \\
\frac{d\alpha_2}{dz} &= \chi (\alpha_1^+ \beta_1 + \alpha_3^+ \beta_2) + \sqrt{\frac{\chi \beta_1}{2}} (\eta_1 - i\eta_6) + \sqrt{\frac{\chi \beta_2}{2}} (\eta_3 + i\eta_7), \\
\frac{d\alpha_2^+}{dz} &= \chi (\alpha_1 \beta_1^+ + \alpha_3 \beta_2^+) + \sqrt{\frac{\chi \beta_1^+}{2}} (\eta_2 + i\eta_5) + \sqrt{\frac{\chi \beta_2^+}{2}} (\eta_4 + i\eta_8), \\
\frac{d\alpha_3}{dz} &= \chi \alpha_2^+ \beta_2 + \sqrt{\frac{\chi \beta_2}{2}} (\eta_3 - i\eta_7), \\
\frac{d\alpha_3^+}{dz} &= \chi \alpha_2 \beta_2^+ + \sqrt{\frac{\chi \beta_2^+}{2}} (\eta_4 - i\eta_8), \\
\frac{d\beta_1}{dz} &= -\chi \alpha_1 \alpha_2, \\
\frac{d\beta_1^+}{dz} &= -\chi \alpha_1^+ \alpha_2^+, \\
\frac{d\beta_2}{dz} &= -\chi \alpha_2 \alpha_3, \\
\frac{d\beta_2^+}{dz} &= -\chi \alpha_2^+ \alpha_3^+,
\end{aligned} \tag{27}$$

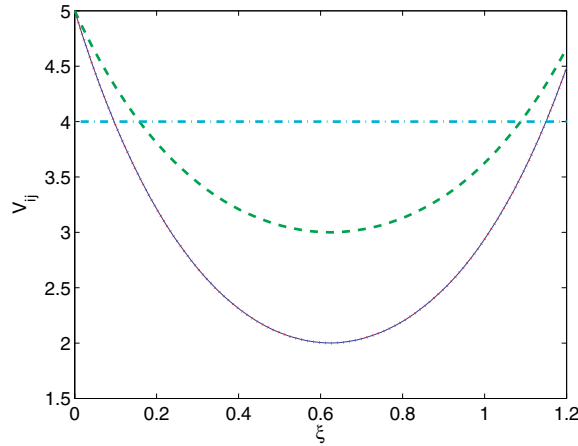


**Figure 6.** Positive- $P$  solution averaged over  $2.68 \times 10^6$  stochastic trajectories for the tripartite entanglement criteria with the doubly concurrent Hamiltonian of section 3.2. The solid line is  $V_{12}$  and  $V_{23}$ , while the dashed line is  $V_{13}$ . The horizontal axis is the scaled interaction length,  $\xi = |\beta_0|\chi z$ .

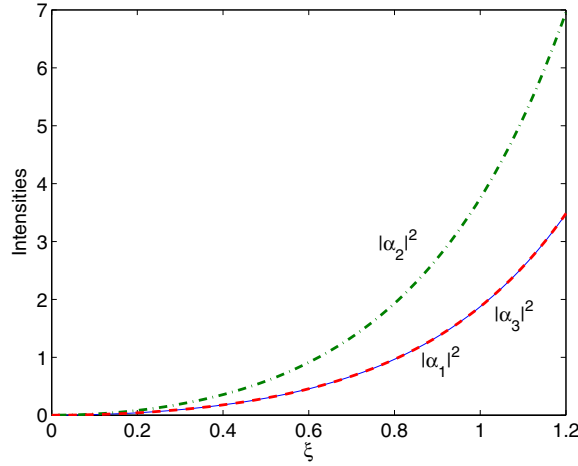


**Figure 7.** Output intensities for the same system and parameters as figure 6.

where the real Gaussian noise terms have the correlations

$$\overline{\eta_j(z)} = 0, \quad \overline{\eta_j(z)\eta_k(z')} = \delta_{jk}\delta(z - z'). \quad (28)$$

As in the previous section, stochastic averages of products of the variables represent normally ordered operator expectation values, with there being correspondences between  $\alpha_j, \alpha_j^\dagger, \beta_j, \beta_j^\dagger$  and  $\hat{a}_j, \hat{a}_j^\dagger, \hat{b}_j, \hat{b}_j^\dagger$ .

The results of stochastic integration of (27) are shown in figure 6 for the tripartite entanglement criteria, for parameter values  $\chi = 10^{-2}, \beta_1(0) = \beta_2(0) = 10^3$  and  $\alpha_1(0) = \alpha_2(0) = \alpha_3(0) = 0$ . We see that the correlations are not symmetric, but that tripartite entanglement is available. The output intensities are shown in figure 7, from which we again see that the inequalities are violated for relatively weak fields. For this system, the analytic results which we presented above give the same results as the stochastic integration over the interaction range shown.

#### 4. Doubled intracavity nonlinearities

Now that we have demonstrated that the two Hamiltonians of section 3 can produce entanglement, we will examine the more realistic physical situations where the processes described happen inside pumped optical cavities. As optical cavities can be tuned to be resonant with only a certain number of modes, a fuller description of the physics involved can be given in a simple manner.

##### 4.1. Cascaded nonlinearities in a cavity

To consider the scheme described by the interaction Hamiltonian of (4) inside a resonant pumped optical cavity, we must add terms to the Hamiltonian, so that

$$H = H_{\text{int}} + H_{\text{pump}} + H_{\text{damp}}, \quad (29)$$

where  $H_{\text{int}}$  has the same form as the interaction Hamiltonian of (4), and

$$\begin{aligned} H_{\text{pump}} &= i\hbar(\epsilon_1 \hat{b}_1^\dagger + \epsilon_2 \hat{b}_2^\dagger) + \text{h.c.}, \\ H_{\text{damp}} &= \hbar \left( \sum_k \hat{\Gamma}_{a,k}^k \hat{a}_k^\dagger + \sum_j \hat{\Gamma}_b^j \hat{b}_j^\dagger \right) + \text{h.c.}, \end{aligned} \quad (30)$$

where  $k = 1, 2, 3$  and  $j = 1, 2$ . In the above,  $\epsilon_j$  are the classical pump amplitudes at the two input frequencies and  $\hat{\Gamma}_{a,b}^k$  are bath operators. The field operators now refer to the intracavity fields. This now becomes equivalent to the scheme of Guo *et al* [5], who analysed it using quantum Langevin equations in an undepleted pump approximation. Following the same procedures used in deriving (17) and making the usual zero-temperature Markovian bath approximation, we find the positive- $P$  equations which give a full quantum description of this system,

$$\begin{aligned} \frac{d\alpha_1}{dt} &= -\gamma_1 \alpha_1 + \chi_1 \alpha_2^+ \beta_1 + \sqrt{\frac{\chi_1 \beta_1}{2}} (\eta_1 + i\eta_3), \\ \frac{d\alpha_1^+}{dt} &= -\gamma_1 \alpha_1^+ + \chi_1 \alpha_2 \beta_1^+ + \sqrt{\frac{\chi_1 \beta_1^+}{2}} (\eta_2 + i\eta_4), \\ \frac{d\alpha_2}{dt} &= -\gamma_2 \alpha_2 + \chi_1 \alpha_1^+ \beta_1 - \chi_2 \alpha_3 \beta_2^+ + \sqrt{\frac{\chi_1 \beta_1}{2}} (\eta_1 - i\eta_3) - \sqrt{\frac{\chi_2 \alpha_3}{2}} (\eta_7 - i\eta_5), \\ \frac{d\alpha_2^+}{dt} &= -\gamma_2 \alpha_2^+ + \chi_1 \alpha_1 \beta_1^+ - \chi_2 \alpha_3^+ \beta_2 + \sqrt{\frac{\chi_1 \beta_1^+}{2}} (\eta_2 - i\eta_4) - \sqrt{\frac{\chi_2 \alpha_3^+}{2}} (\eta_8 - i\eta_6), \\ \frac{d\alpha_3}{dt} &= -\gamma_3 \alpha_3 + \chi_2 \alpha_2 \beta_2, \\ \frac{d\alpha_3^+}{dt} &= -\gamma_3 \alpha_3^+ + \chi_2 \alpha_2^+ \beta_2^+, \\ \frac{d\beta_1}{dt} &= \epsilon_1 - \kappa_1 \beta_1 - \chi_1 \alpha_1 \alpha_2, \\ \frac{d\beta_1^+}{dt} &= \epsilon_1^* - \kappa_1 \beta_1^+ - \chi_1 \alpha_1^+ \alpha_2^+, \\ \frac{d\beta_2}{dt} &= \epsilon_2 - \kappa_2 \beta_2 - \chi_2 \alpha_2 \alpha_3^+ + \sqrt{\frac{\chi_2 \alpha_3}{2}} (\eta_7 + i\eta_5), \\ \frac{d\beta_2^+}{dt} &= \epsilon_2^* - \kappa_2 \beta_2^+ - \chi_2 \alpha_2^+ \alpha_3 + \sqrt{\frac{\chi_2 \alpha_3^+}{2}} (\eta_8 + i\eta_6). \end{aligned} \quad (31)$$

Note that the correlations of the noise terms are now in time rather than in the spatial variable. These equations can be integrated numerically in any parameter regime, including near to any critical points of the system. However, as we will not be concerned with the behaviour of this system in the neighbourhood of any critical points, we will proceed via a linearized fluctuation analysis. This involves separating the variables of the positive- $P$  equations into their mean-field steady-state solutions plus a fluctuating part, e.g.  $\alpha_1 = \alpha_1^{\text{ss}} + \delta\alpha_1$ . Solving the classical equations of motion to find the steady-state solutions, we may then write equations for the fluctuations from which we can calculate the output spectral quantities of interest [23]. Neglecting the noise terms in (31), we find the following classical equations for the interacting fields:

$$\begin{aligned}\frac{d\alpha_1}{dt} &= -\gamma_1\alpha_1 + \chi_1\alpha_2^*\beta_1, & \frac{d\alpha_2}{dt} &= -\gamma_2\alpha_2 + \chi_1\alpha_1^*\beta_1 - \chi_2\alpha_3\beta_2^*, \\ \frac{d\alpha_3}{dt} &= -\gamma_3\alpha_3 + \chi_2\alpha_2\beta_2, & \frac{d\beta_1}{dt} &= \epsilon_1 - \kappa_1\beta_1 - \chi_1\alpha_1\alpha_2, \\ \frac{d\beta_2}{dt} &= \epsilon_2 - \kappa_2\beta_2 - \chi_2\alpha_2\alpha_3^*,\end{aligned}\quad (32)$$

where  $\gamma_j(\kappa_j)$  are the cavity damping rates for  $\alpha_j(\beta_j)$ .

We see that one possible set of solutions to these equations is

$$\alpha_j^{\text{ss}} = 0, \quad (33)$$

$$\beta_j^{\text{ss}} = \epsilon_j/\kappa_j, \quad (34)$$

which are reminiscent of those found for the well-known OPO below threshold. To examine the stability of these solutions, we write the linearized equation for the fluctuations,

$$d\delta\tilde{\alpha} = A\delta\tilde{\alpha} dt + B dW, \quad (35)$$

where  $\tilde{\alpha} = [\delta\alpha_1, \delta\alpha_1^+, \delta\alpha_2, \delta\alpha_2^+, \delta\alpha_3, \delta\alpha_3^+, \delta\beta_1, \delta\beta_1^+, \delta\beta_2, \delta\beta_2^+]^T$ ,  $B$  is the matrix of the noise terms of (17), but with the classical steady-state solutions used in place of the stochastic variables and  $dW$  is a vector of Wiener increments. The drift matrix is found as

$$A = [A_1 \ A_2], \quad (36)$$

where

$$A_1 = \begin{bmatrix} -\gamma_1 & 0 & 0 & \chi_1\beta_1^{\text{ss}} & 0 & 0 \\ 0 & -\gamma_1 & \chi_1(\beta_1^*)^{\text{ss}} & 0 & 0 & 0 \\ 0 & \chi_1\beta_1^{\text{ss}} & -\gamma_2 & 0 & -\chi_2(\beta_2^*)^{\text{ss}} & 0 \\ \chi_1(\beta_1^*)^{\text{ss}} & 0 & 0 & -\gamma_2 & 0 & -\chi_2\beta_2^{\text{ss}} \\ 0 & 0 & \chi_2\beta_2^{\text{ss}} & 0 & -\gamma_3 & 0 \\ 0 & 0 & 0 & \chi_2(\beta_2^*)^{\text{ss}} & 0 & -\gamma_3 \\ -\chi_1\alpha_2^{\text{ss}} & 0 & -\chi_1\alpha_1 & 0 & 0 & 0 \\ 0 & -\chi_1(\alpha_2^*)^{\text{ss}} & 0 & -\chi_1(\alpha_1^*)^{\text{ss}} & 0 & 0 \\ 0 & 0 & -\chi_2(\alpha_3^*)^{\text{ss}} & 0 & 0 & -\chi_2\alpha_2^{\text{ss}} \\ 0 & 0 & 0 & -\chi_2\alpha_3^{\text{ss}} & -\chi_2(\alpha_2^*)^{\text{ss}} & 0 \end{bmatrix} \quad (37)$$

and

$$A_2 = \begin{bmatrix} \chi_1(\alpha_2^*)^{\text{ss}} & 0 & 0 & 0 \\ 0 & \chi_1\alpha_2^{\text{ss}} & 0 & 0 \\ \chi_1(\alpha_1^*)^{\text{ss}} & 0 & 0 & -\chi_2\alpha_3^{\text{ss}} \\ 0 & \chi_1\alpha_1^{\text{ss}} & -\chi_2(\alpha_3^*)^{\text{ss}} & 0 \\ \chi_2\alpha_2^{\text{ss}} & 0 & 0 & 0 \\ 0 & \chi_2(\alpha_2^*)^{\text{ss}} & 0 & 0 \\ -\kappa_1 & 0 & 0 & 0 \\ 0 & -\kappa_1 & 0 & 0 \\ 0 & 0 & -\kappa_2 & 0 \\ 0 & 0 & 0 & -\kappa_2 \end{bmatrix}. \quad (38)$$

As long as none of the eigenvalues of this drift matrix has a positive real part, the solutions are stable and the linearized fluctuation analysis should be valid. Although general analytical expressions for the eigenvalues can be found, these are rather complicated. In the simplifying case below threshold where we set the output loss rates equal,  $\gamma_j = \gamma$  and  $\kappa_j = \kappa$ , we find a degenerate eigenvalue which can be positive,

$$\lambda = -\gamma + \frac{\sqrt{\chi_1^2\epsilon_1^2 - \chi_2^2\epsilon_2^2}}{\kappa}. \quad (39)$$

This eigenvalue sets a condition for the relative strengths of the pump,

$$\chi_1^2\epsilon_1^2 - \chi_2^2\epsilon_2^2 < \gamma^2\kappa^2. \quad (40)$$

When this condition is violated, the below threshold solutions are unstable.

The spectral correlations are found in the normal manner, via the equation

$$S(\omega) = (A + i\omega)^{-1} D (A^T - i\omega)^{-1}, \quad (41)$$

where  $D$  is the diffusion matrix with the steady-state values of the fields and the standard input–output relationships [24]. We will denote the output spectral correlations equivalent to  $V_{ij}$  of (2) as  $S_{ij}$ . Although we were able to find analytic expressions for the correlations, these were extremely complicated and gave little insight, therefore we have presented numerical results in figure 8. Our numerical investigations over a range of parameters did not find any violation of the inequalities noticeably better than that presented. We found that when the pumping rates increase above the value of  $\epsilon_j = \gamma\kappa/\chi_j$ , the violations rapidly disappear. What is immediately visible is that the inequalities are not all violated equally, although true tripartite entanglement is demonstrated. We note that numerical investigations show that this system exhibits a range of behaviours, with self-pulsing type oscillations and possible bistability for particular parameter regimes, but here we are only interested in its suitability as a source of tripartite entanglement and an investigation of these effects is outside the scope of this work.

#### 4.2. Intracavity concurrent twin nonlinearities

In a similar manner to the preceding (section 4.1), we will now investigate the performance of an intracavity version of the system described by (19). We again find the classical equations

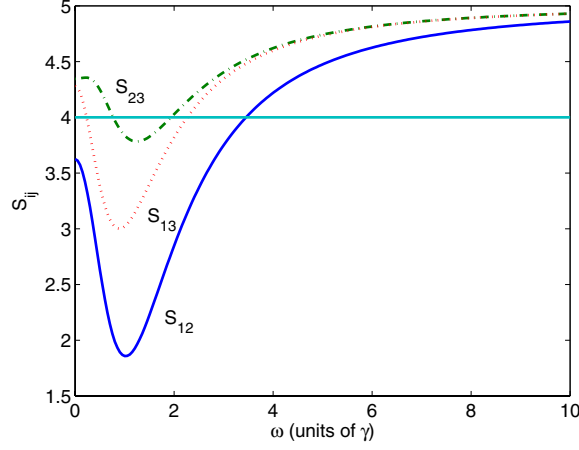


**Figure 8.** Tripartite entanglement criteria for the system of section 4.1, for  $\kappa = \gamma = 1$ ,  $\chi_1 = \chi_2 = 10^{-2}$  and  $\epsilon_1 = \epsilon_2 = 0.9\gamma\kappa/\chi_1$ .

by dropping the noise terms in the appropriate positive- $P$  equations and solve these for the mean fields in the steady state. The equations for the mean fields are

$$\begin{aligned} \frac{d\alpha_1}{dt} &= -\gamma_a\alpha_1 + \chi\alpha_2^*\beta_1, & \frac{d\alpha_2}{dt} &= -\gamma_a\alpha_2 + \chi(\alpha_1^*\beta_1 + \alpha_3^*\beta_2), \\ \frac{d\alpha_3}{dt} &= -\gamma_a\alpha_3 + \chi\alpha_2^*\beta_2, & \frac{d\beta_1}{dt} &= \epsilon_1 - \gamma_b\beta_1 - \chi\alpha_1\alpha_2, \\ \frac{d\beta_2}{dt} &= \epsilon_2 - \gamma_b\beta_2 - \chi\alpha_2\alpha_3, \end{aligned} \quad (42)$$

where  $\gamma_{a,b}$  are the cavity damping rates for the appropriate modes and  $\epsilon_j$  are the classical pumping terms. Although we have chosen the simple case where both pump modes have the same loss rate, as do the three signal modes, this is not essential, although it does serve to simplify our analysis. We may now solve the above equations to find the steady-state mean-field solutions and the conditions for the stability of the linearized fluctuation analysis.

To find analytical expressions, we will set  $\epsilon_1 = \epsilon_2 = \epsilon$ . We find that there is an oscillation threshold at the value  $\epsilon_{\text{th}} = \gamma_a\gamma_b/2\chi$ , below which  $\alpha_1^{\text{ss}} = \alpha_2^{\text{ss}} = \alpha_3^{\text{ss}} = 0$  and  $\beta_1^{\text{ss}} = \beta_2^{\text{ss}} = \epsilon/\gamma_b$ . Above this threshold, we find

$$\alpha_2^{\text{ss}} = \pm\sqrt{\frac{2}{\chi}(\epsilon - \epsilon_{\text{th}})}, \quad \alpha_1^{\text{ss}} = \alpha_3^{\text{ss}} = \pm\sqrt{\frac{1}{\chi}(\epsilon - \epsilon_{\text{th}})}, \quad \beta_1^{\text{ss}} = \beta_2^{\text{ss}} = \frac{\gamma_a}{2\chi}, \quad (43)$$

where all  $\alpha_j$  must have the same sign. What is unusual about this system in comparison with the normal optical parametric oscillator is that it is stable at threshold, with the critical point for the below threshold solutions being at a pump amplitude of  $\epsilon_c = \gamma_a\gamma_b/\sqrt{2}\chi$ , which means that  $\epsilon_c = \sqrt{2}\epsilon_{\text{th}}$ . For this pumping strength, the actual above threshold solutions are stable, so that this system, at least for the parameter regimes we consider here, is always stable. With these steady-state solutions, we have all the information we need to calculate the output spectral correlations of interest.

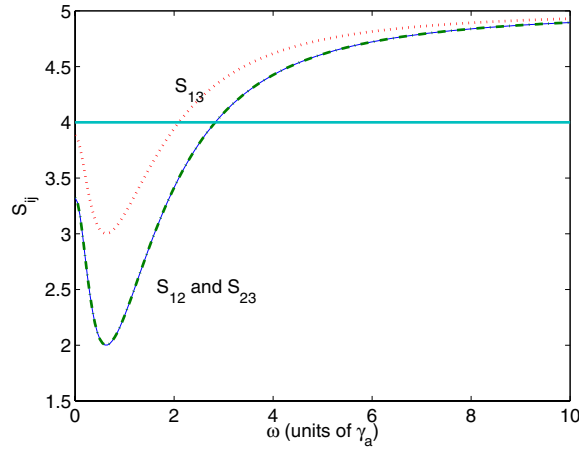


**Figure 9.** Tripartite entanglement criteria for the system of section 4.2, for  $\gamma_a = \gamma_b = 1$ ,  $\chi = 10^{-2}$  and  $\epsilon = 0.9\epsilon_{\text{th}}$ .

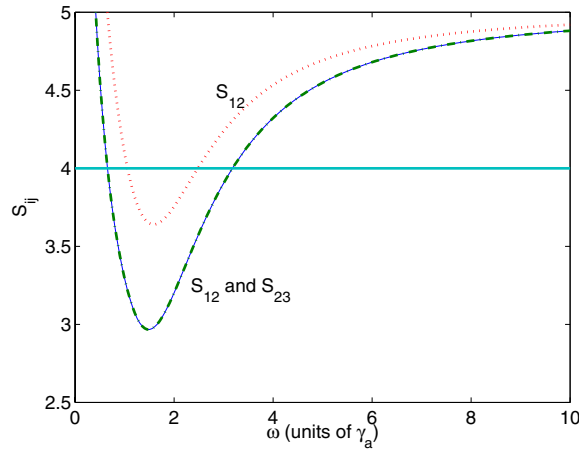


**Figure 10.** Tripartite entanglement criteria for the system of section 4.2, for  $\gamma_a = \gamma_b = 1$ ,  $\chi = 10^{-2}$  and  $\epsilon = 2\epsilon_{\text{th}}$ .

Below the oscillation threshold, we can find relatively simple expressions for the output spectral correlations,

$$\begin{aligned}
 S_{12}(\omega) = S_{23}(\omega) &= 5 - \frac{24\gamma_a\gamma_b\chi\epsilon(\gamma_a^2\gamma_b^2 - 3\gamma_a\gamma_b\chi\epsilon + 2\chi^2\epsilon^2 + \gamma_b^2\omega^2)}{\gamma_a^4\gamma_b^4 + (2\chi^2\epsilon^2 + \gamma_b^2\omega^2)^2 + 2\gamma_a^2\gamma_b^2(\gamma_b^2\omega^2 - 2\chi^2\epsilon^2)}, \\
 S_{13}(\omega) &= 5 - \frac{16\gamma_a\gamma_b\chi\epsilon(\gamma_a^2\gamma_b^2 - 3\gamma_a\gamma_b\chi\epsilon + 2\chi^2\epsilon^2 + \gamma_b^2\omega^2)}{\gamma_a^4\gamma_b^4 + (2\chi^2\epsilon^2 + \gamma_b^2\omega^2)^2 + 2\gamma_a^2\gamma_b^2(\gamma_b^2\omega^2 - 2\chi^2\epsilon^2)},
 \end{aligned} \tag{44}$$

whereas above threshold the analytical expressions become more complicated.

We show results for the tripartite criteria in figure 9 immediately below the oscillation threshold and in figure 10 for  $\epsilon = 2\epsilon_{\text{th}}$ . We find that the violations of the inequalities are strongest at threshold, with  $S_{12} = S_{23}$  and  $S_{13}$  showing a lesser violation of the criterion. We

also found that, well above threshold, the individual quadratures  $X_1$  and  $X_3$  become squeezed, although  $X_2$  remains above the shot-noise level.

## 5. Conclusions

We have examined two different interaction schemes in terms of their potential for creating continuous variable tripartite entanglement. We have used a set of inequalities whose violation is sufficient to show that genuine tripartite entanglement is present. One of the schemes is based on two cascaded nonlinearities and the other on two concurrent nonlinearities. Although the scheme based on cascaded linearities has been analysed previously, we have extended these analyses to include depletion of the pumping fields in a full quantum treatment. Both these schemes were shown to exhibit a good degree of violation of the van Loock and Furusawa inequalities, and are therefore suitable candidates for practical applications. The concurrent scheme has the possible advantage that two of the outputs are of equal intensity and is symmetric in two of the correlations, whereas the cascaded scheme produces three different intensities and all three correlations give different values. Although both schemes perform well, which one is preferable in a given situation may come down to the preferences and experiences of the experimenters wishing to use them.

## Acknowledgments

This research was supported by the Australian Research Council and the Queensland State Government.

## References

- [1] Giedke G, Kraus B, Lewenstein M and Cirac J I 2001 *Phys. Rev. A* **64** 052303
- [2] van Loock P and Furusawa A 2003 *Phys. Rev. A* **67** 052315
- [3] Jing J, Zhang J, Yan Y, Zhao F, Xie C and Peng K 2003 *Phys. Rev. Lett.* **90** 167903
- [4] Aoki T, Takei N, Yonezawa H, Wakui K, Hiraoka T and Furusawa A 2003 *Phys. Rev. Lett.* **91** 080404
- [5] Guo J, Zou H, Zhai Z, Zhang J and Gao J 2005 *Phys. Rev. A* **71** 034305
- [6] Ferraro A, Paris M G A, Bondani M, Allevi A, Puddu E and Andreoni A 2004 *J. Opt. Soc. Am. B* **21** 1241
- [7] Bradley A S, Olsen M K, Pfister O and Pooser R C 2005 *Phys. Rev. A* **72** 053805
- [8] Duan L M, Giedke G, Cirac J I and Zoller P 2000 *Phys. Rev. Lett.* **84** 2722
- [9] Simon R 2000 *Phys. Rev. Lett.* **84** 2726
- [10] Greenberger D M, Horne M A and Zeilinger A 1989 *Bell's Theorem, Quantum Theory, and Conceptions of the Universe* ed M Kafatos (Dordrecht: Kluwer)
- [11] Greenberger D M, Horne M A, Shimony A and Zeilinger A 1990 *Am. J. Phys.* **58** 1131
- [12] Drummond P D 1990 *Phys. Rev. A* **42** 6845
- [13] Smithers M E and Lu E Y C 1974 *Phys. Rev. A* **10** 1874
- [14] Ferraro A and Paris M G A 2005 *J. Opt. B: Quantum Semiclass. Opt.* **7** 174
- [15] Olsen M K, Horowicz R J, Plimak L I, Treps N and Fabre C 2000 *Phys. Rev. A* **61** 021803
- [16] Olsen M K, Plimak L I and Khoury A Z 2003 *Opt. Commun.* **215** 101
- [17] Olsen M K 2004 *Phys. Rev. A* **70** 035801
- [18] Huttner B, Serulnik S and Ben-Aryeh Y 1990 *Phys. Rev. A* **42** 5594
- [19] Caves C M and Crouch D D 1987 *J. Opt. Soc. Am. B* **4** 1535
- [20] Drummond P D and Gardiner C W 1980 *J. Phys. A: Math. Gen.* **13** 2353
- [21] Shen Y R 1967 *Phys. Rev.* **155** 921
- [22] Gardiner C W 1991 *Quantum Noise* (Berlin: Springer)
- [23] Walls D F and Milburn G J 1994 *Quantum Optics* (Berlin: Springer)
- [24] Gardiner C W and Collett M J 1985 *Phys. Rev. A* **31** 3761